Published in final edited form as:

Vet Ophthalmol. 2019 May ; 22(3): 345–352. doi:10.1111/vop.12600.

Mapping the entire nerve architecture of the cat cornea

Jiucheng He, MD, PhD[1,2], **Thang Luong Pham, MS**[1], and **Haydee E.P. Bazan, PhD**[1,2,*]

[1]Neuroscience Center of Excellence, School of Medicine, Louisiana State University Health New Orleans, New Orleans, Louisiana, USA.

[2]Department of Ophthalmology, School of Medicine, Louisiana State University Health New Orleans, New Orleans, Louisiana, USA.

Abstract

Objective.—To provide a complete nerve architecture and neuropeptide distribution in the cat cornea.

Animals studied.—Two adult domestic cats.

Procedure.—The cat corneas were stained with protein gene product (PGP) 9.5 antibody – a pan marker for nerve fibers – then divided into four quarters and double labeled with calcitonin gene-related peptide (CGRP) or substance P (SP) antibodies. Relative corneal nerve fiber densities and nerve terminals were evaluated in whole mount images by computer-assisted analysis.

Results.—An average of 21.5 ± 2.1 thick stromal nerves enter the cornea around the limbus where they split into many branches going up to the anterior stroma. Some branches link to each other, but most of them penetrate the basement membrane in the periphery to give origin to subbasal bundles, which run centripetally and merge to form a whirl-like structure (vortex) at the center. These nerve bundles send out many fine terminals that innervate the epithelial cells. Subbasal nerve density and nerve terminals were greater in the center than in the periphery of the cornea. Additionally, CGRP-positive central epithelial nerve fibers and terminals were more abundant than SP-positive nerves and terminals.

Conclusion.—The architecture of cat corneal nerves shows similarities to human and mouse cornea innervation. This study provides useful data for researchers who use the cat model to assess corneal nerve pathological alterations, as well as in the veterinary field where corneal opacities, ulcerations, and infections damage the nerves and decrease sensitivity.

Keywords

cat; corneal innervation; sensory nerves; substance P; calcitonin gene-related peptide; immunofluorescence

*Correspondence to: Haydee E.P. Bazan, Neuroscience Center of Excellence and Department of Ophthalmology, School of Medicine, Louisiana State University Health, New Orleans, Louisiana, United States 70112; Phone: 504-599-0877; Fax: 504-568-5801; hbazan1@lsuhsc.edu.

Introduction

The cornea – a naturally transparent tissue – does not contain blood vessels but is rich in nerves. Early retrograde-tracing studies have demonstrated that the mammalian cornea is densely packed with sensory nerves derived from the ophthalmic division of the trigeminal ganglion – autonomic parasympathetic fibers from the ciliary ganglion – and a small number of sympathetic nerves from the superior cervical ganglion. [1,2] Corneal nerves play an important role in the regulation of corneal epithelial integrity, proliferation, and wound healing; damage of the nerves causes an alteration in epithelial morphology and function, poor tear-film production, and delays wound healing. [3–5] The resulting neurotrophic keratitis and corneal opacity reduce corneal transparency and impair vision.

Cats have been used to study several physiological functions of the corneal endothelium as their limited regenerative capacity parallels that of humans. [6,7] The cat cornea responds to mechanical, chemical, and thermal stimuli and has been widely employed to study pain response following corneal injury, demonstrating a similar pain response as that found in human cornea. [8–11] Early studies have shown innervation of the cat cornea employing histological staining with gold chloride solution [12] and more recently by *in vivo* confocal microscopy to provide an anatomical reference for veterinary use [13,14] as well as to investigate nerve regeneration after lamellar keratectomy. [15] However, the detailed nerve architecture and neuropeptide distribution in the cat cornea have not been reported. In this study, we used our modified method of immunofluorescence and imaging [16,17] to characterize the entire nerve architecture as well as the distribution of two main sensory neuropeptides calcitonin gene-related peptide (CGRP) and substance P (SP) in an attempt to provide some useful information for clinicians and researchers who use cat models to assess corneal nerve pathology.

Materials and Methods

Immunofluorescence staining and imaging

Four fresh corneas removed from two female domestic cats that died in traffic accidents were used in the study. According to the owners, the cats were 16 and 23 months old. The eyes were enucleated following death, immediately immersed in ice, and transported to the laboratory. The corneas were cut along the corneoscleral limbus and fixed in freshly prepared 2% paraformaldehyde in 0.01M phosphate buffer (PH 7.4) for 2 hours at room temperature. Corneas were washed thoroughly with 1X PBS (three times for 15 min each) and incubated with 10% goat serum in 0.01M PBS for 1 hour at room temperature (RT) to block nonspecific staining. Afterward, the corneas were incubated in a 24-well plate (1 cornea per well) with rabbit monoclonal anti-protein gene product 9.5 (PGP9.5, EPR4118) antibody (1:1500, Abcam Inc. Cambridge, MA) in 0.01M PBS containing 1.5% normal goat serum plus 0.3% Triton X-100 for 72 hours at RT with constant shaking. After washings with PBS (three times for 15 min each), the corneas were incubated with the secondary antibody Alexa Fluor® 488 goat anti-rabbit Ig G (H+L) (1:1500, Thermo Fisher Scientific, Waltham, MA) for 24 hours at RT and washed thoroughly with PBS. To exclude non-specific labeling, the primary antibody was replaced by serum IgG of the same host species.

For double immunofluorescence, after finishing the labeling with the first set of antibodies (PGP9.5 and correspondent secondary antibodies), the corneas were cut into four equal quarters; two quarters were used for CGRP staining and the other two for SP staining. Tissues were incubated with the second primary antibodies mouse monoclonal anti-CGRP (1:800, Abcam Inc. Cambridge, MA) or rat monoclonal anti-SP (1:100, Santa Cruz Inc., CA) for 72 hours at RT followed by a corresponding tetramethylrhodamine isothiocyanate (TRITC)-conjugated secondary antibody (1:1500); washings were performed in the same manner as described above. Images were recorded with a fluorescent microscope (Olympus IX71; Olympus Corp., Tokyo, Japan). Entire whole-mount views of corneal nerves were built at different layers including superficial terminals, subbasal bundles, and stromal nerve trunks. For better contrast, the color images were switched to black and white, with a black background and then inverted to a white background. [16,17] For transected images of corneal nerves, 15 μm cryostat sagittal sections were prepared from the samples after finishing the whole mount examination using the same method as described previously. [16,17]

Data analysis

To investigate the distribution of epithelial nerves, the corneas were divided into central and peripheral zones. The central zone was defined by a radius of 3mm starting at the apex, and the peripheral zone with a radius of 3mm beginning at the limbus, leaving 2 mm of space between the two zones uncounted to avoid overlap. To compare the densities of the epithelial nerves, four images for each zone were randomly chosen from each cornea (1 image/quadrant). The images were recorded with a 10x objective lens. A total of 16 images for each zone from 4 corneas were averaged. Nerve terminals in the superficial epithelia within the central and peripheral zones were calculated by directly counting the number of terminals in each image. Sixteen images per zone from 4 corneas were analyzed. The terminal numbers in each image were counted using the Image J software (NIH). Since each image comprised an area of 0.59 mm^2, the terminal numbers per square millimeter were calculated.

To obtain the relative content of neuropeptides, the corneas were double labeled with PGP9.5 and CGRP or SP. For each neuropeptide, a total of 16 images were taken at an objective lens with a 10x magnification from the center of the four corneas. Afterward, in the same visual field, the same number of images for PGP9.5 (which represents the total nerve content) were taken.

The nerve fibers in each image were carefully drawn with 4-pixel lines following the course of each fiber by using the brush tool in Photoshop™ imaging software. The percentage of nerve area was quantified for each image. At the same visual field, PGP9.5 equaled the percentage of total nerve area, and the average ratio of the peptide-positive nerve area against PGP9.5 represented the relative content of each neuropeptide.

Results

Stromal nerve architecture

There were an average of 21.5 ± 2.1 thick stromal nerves that entered into the cornea around the limbus. Stromal nerve trunks divide into many branches (Figure 1) that run toward the center and go up to the anterior stroma. Some of the branches connect with each other to constitute the stromal nerve network, but most of them penetrate the basement membrane to form the subbasal nerves.

Epithelial nerve architecture

The epithelial nerves derive from the tips of stromal nerve branches. In the adult cat, the tips are predominantly located in the peripheral zone where they form the long subbasal nerve bundles that run centripetally and converge into a whirl-like structure or vortex in the central area close to the corneal apex (Figure 2A). In the four corneas examined, each cornea had only one vortex. One of the vortexes ran clockwise, and the other three ran in a counter-clockwise pattern (Figure 2B). From periphery to center, the long epithelial nerve bundles produced a dense net of smaller nerves, which connect with each other and constitute the epithelial nerve network. Along the path of nerve fibers, the bundles give off many superficial fine terminals to innervate the epithelial cells (Figure 2B). The shape and density of terminals differ from the periphery to the center. In the peripheral area, the terminals are longer with more divisions but are less densely distributed than those in the center and the vortex.

The subbasal nerve density (Figure 3A), calculated as the percentage of total area, was 23.7 ± 3.8% in the central area and 9.8 ± 2.9% in the peripheral area, with a significant difference of $p<0.001$. Similarly, nerve terminals (Figure 3B), calculated from 32 images (16 images per zone) of 4 eyes as the average number of nerve terminals/mm^2 were also greater in the center (1,011 ± 260) than in the periphery (441 ± 116, $p< 0.005$).

CGRP and SP content of central corneal nerves

In the central zone, CGRP-positive nerve fibers constituted 26.5 ± 4.9% of the total subbasal nerve content double stained with PGP9.5. Corneas double stained with PGP9.5 and SP show significantly less percent of SP-positive nerves than CGRP with 19.7 ± 3.3%, ($p<0.001$, Figure 4A). As a consequence, the percentage of CGRP-positive nerve terminals was higher (49.7 ± 6.3%) than the percentage of SP-positive terminals (37.1 ± 5.7%, $p<0.05$, Figure 4B). Representative whole-mount and cross-section images of double staining with PGP9.5 and CGRP or SP of cat subbasal nerve bundles and terminals in the center area are shown in Figures 5A and5B.

Discussion

Cat corneal innervation has been studied already by immunochemical methods, [1,2,12] and, more recently, by *in vivo* confocal microscopy, [13,14] but none of these studies have provided an entire map of the innervation or the content of the most abundant neuropeptides, CGRP and SP. Using a modified method of immunofluorescence and imaging developed in

our laboratory, we previously unveiled the entire human corneal nerve architecture [16] and studied the changes that occur during diabetes and corneal dystrophies. [4,18] In the present study, we used this technique to provide, for the first time, an entire view of the cat corneal nerve architecture, including epithelial terminals, subbasal bundles, and stromal nerve trunks. We also determined the relative contents of the two main sensory neuropeptides, CGRP and SP.

Our studies show that corneal innervation in the adult cat shares many common features with humans. As with humans, [4,16] cat nerves reach the cornea through the limbal area of the stroma. These nerves entered the cornea in a radial pattern, subsequently dividing into smaller branches like a tree. Some branches connected at the center of the stroma to form a stromal nerve network, but most penetrated upward to give birth to the epithelial nerve bundles. There were no obvious differences observed between nerve densities in the four corneal quadrants. Epithelial nerves come from the tips of stromal nerve branches, which penetrate the basement membrane to the subbasal layer. The tips are predominantly present in the peripheral cornea. Generally, one tip gives off several subbasal bundles. The long bundles run from the periphery and converge into the central area to form the whorl-like structure or vortex. Along the path of the subbasal nerve fiber bundle, many smaller nerve fibers are produced, which connect with each other to form a subbasal nerve network. Fine terminals or free endings originated from the subbasal nerves innervate the epithelial cells. Similar to human corneas, [16] the density of epithelial nerves, including the subbasal nerves and free endings, are significantly higher in the center than in the periphery. As seen in humans, we observed one vortex per cornea in the four cat corneas analyzed, and the patterns of the vortex included clockwise or counterclockwise, depending on the cat. This is different from the mouse or rabbit. [17,19] In the mouse, 18% of the eyes have more than one vortex per cornea, [17] while, in rabbit, corneal nerves do not have a vortex. [19]

Most corneal nerve fibers are sensory in origin and are derived from the ophthalmic branch of the trigeminal ganglion. [1,2] CGRP and SP are the two main sensory neuropeptides found in corneal nerves [3,17] and have been shown to induce epithelial cell proliferation, migration and adhesion, promote wound healing [20–22] and modulate tear production and mucus secretion from the goblet cells. [23,24] These sensory neuropeptides have been studied previously by immunohistochemistry in a wide range of animal species, but only a few studies have reported their relative contents in corneas. The proportion of CGRP in the cat cornea is significantly higher than that of SP-positive fibers, which is consistent with what has previously been found in mouse and rabbit, but the relative contents of both CGRP and SP are less than those in mouse and higher than those in rabbit. [17,25] An early study in dogs has shown that both CGRP- and SP-positive nerve fibers make up 99% of the total corneal innervation. [26] In the cat, CGRP- and SP-positive nerves account for about 47% of the total corneal innervation, suggesting that the content of these neuropeptide nerve fibers is related to the animal species.

This result also indicates that in addition to CGRP and SP, cat corneal nerves contain a large number (53%) of other neuropeptides. Those may include other sensory neuropeptides such as galanin [27] and pituitary adenylate cyclase-activating peptide; [28] sympathetic neurotransmitters such as noradrenaline, serotonin and/or neuropeptide Y, [29–31] and the

peptidergic content of corneal parasympathetic nerves such as vasoactive intestinal polypeptide (VIP), met-enkephalin, NPY, and galanin. [27]

Cats often suffer from herpetic keratitis, [32] an ocular surface disease known to damage corneal nerves. [19,33,34] Our previous studies have shown in rabbits and mice that topical treatment with a combination of the neurotrophic factor pigment epithelium-derived factor (PEDF) and the omega-3 fatty acid docosahexaenoic acid (DHA) stimulates the nerve regeneration after refractive surgery, diabetes, and herpesvirus-1 infection. [35–37] Recent studies to uncover the mechanism show an activation of the PEDF-receptor that enhances the synthesis of docosanoids and neurotrophins. [38] While there are no studies on cat herpetic keratitis, this could represent an important future treatment to improve regeneration of nerves damaged by this disease.

Finally, we should point out the limitations of this study. The data shown here only represents two young female cats. Due to the small sample size, we do not know if the cat's corneal nerve density will decrease with age, as we reported previously in humans. We also cannot determine if there is a difference in nerve density due to gender, although we did not find any difference in previous studies of human and mouse corneas. In addition, the origin of neuropeptides has not been determined in this study. All of these issues are of clinical importance and need to be clarified in future studies. A precise description of cat corneal innervation will increase our understanding of corneal neurobiology and provide useful knowledge for veterinarians in treating cat patients with ocular diseases that damage corneal nerves.

Acknowledgements

We acknowledge support from NIH/NEI grant R01 EY019465 and a grant from the Research to Prevent Blindness (to the LSU Eye Center). The funders had no role in study design, data collection and analysis, decision to publish, or preparation of the manuscript. The content of this manuscript is new as well as the sole responsibility of the authors and does not necessarily represent the official views of the granting agencies.

References

1. Marfurt CF. The central projections of trigeminal primary afferent neurons in the cat as determined by the tranganglionic transport of horseradish peroxidase. Journal of the Comparative Neurology 1981; 203: 785–798.
2. Marfurt CF, Kingsley RE, Echtenkamp SF. Sensory and sympathetic innervation of the mammalian cornea. A retrograde tracing study. Investigative Ophthalmology & Visual Science 1989; 30: 461–71. [PubMed: 2494126]
3. Muller IJ, Marfurt CE, Kruse F, et al. Corneal nerves: structure, contents and function. Experimental Eye Research 2003; 76: 521–542. [PubMed: 12697417]
4. He J, Bazan HE. Mapping the nerve architecture of diabetic human corneas. Ophthalmology 2012; 119: 956–964. [PubMed: 22325488]
5. Shaheen BS, Bakir M, Jain S. Corneal nerves in health and disease. Survey of Ophthalmology 2014; 59: 263–285. [PubMed: 24461367]
6. Van Horn DL, Sendele DD, Seideman S, et al. Regenerative capacity of the corneal endothelium in rabbit and cat. Investigative Ophthalmology & Visual Science 1977; 16: 597. [PubMed: 873721]
7. Bourne WM, Nelson LR, Buller CR, et al. Long-term observation of morphologic and functional features of cat corneal endothelium after wounding. Investigative Ophthalmology & Visual Science 1994; 35: 891–899. [PubMed: 8125752]

8. Gallar J, Pozo MA, Tuckett RP, et al. Response of sensory units with unmyelinated fiber to mechanical, thermal and chemical stimulation of the cat's cornea. Journal of Physiology 1993; 468: 609–622. [PubMed: 8254527]
9. Chen X, Gallar J, Belmonte C. Reduction by anti-inflammatory drugs of the response of corneal sensory nerve fibers to chemical irritation. Investigative Ophthalmology & Visual Science 1997; 38: 1944–1953. [PubMed: 9331258]
10. Chen X, Belmonte C, Rang HP. Capsaicin and carbon dioxide act by distinct mechanism on sensory nerve terminal in the cat cornea. Pain 1997; 70: 23–29. [PubMed: 9106806]
11. Gallar J, Acosta MC, Guitierrez AR, et al. Impulse activity in corneal sensory nerve fibers after photorefractive keratectomy. Investigative Ophthalmology & Visual Science 2007; 48: 4033–4037. [PubMed: 17724184]
12. Tailoi CL. Sensitivity and neural organization of the cat cornea. Investigative Ophthalmology & Visual Science 1989; 30(6): 1075–1082. [PubMed: 2732021]
13. Kafarnik C, Friesche J, Reese S. In vivo confocal microscopy in the normal corneas of cats, dogs and birds. Veterinary Ophthalmology 2007; 10: 222–230. [PubMed: 17565554]
14. Reichard M, Hovakimyan M, Wree A, et al. Comparative *in vivo* confocal microscopical study of the cornea anatomy of different laboratory animals. Current Eye Research 2010; 35: 1072–1080. [PubMed: 20961216]
15. Acosta AC, Espana EM, Stoiber J, et al. Corneal stroma regeneration in felines after supradescemetic keratoprostesis implantation. Cornea 2006; 25: 830–838. [PubMed: 17068461]
16. He J, Bazan NG, Bazan HEP. Mapping the entire human corneal nerve architecture. Experimental Eye Research 2010; 91: 513–523. [PubMed: 20650270]
17. He J, Bazan HEP. Neuroanatomy and neurochemistry of mouse cornea. Investigative Ophthalmology & Visual Science 2016; 57: 664–674. [PubMed: 26906155]
18. He J Bazan HE. Corneal nerve architecture in a donor with unilateral corneal epithelial basement membrane dystrophy. Ophthalmic Research 2013; 49 (1):185–191. [PubMed: 23306594]
19. He J, Cosby R, Hill JM, et al. Changes in corneal innervation after HSV-1 latency established with different reactivation phenotypes. Current Eye Research 2017; 42: 181–186. [PubMed: 27315102]
20. Mikulec AA, Tanelian DL. CGRP increases the rate of corneal re-epithelialization in an in vitro whole mount preparation. J Ocul Pharmacol Ther. 1996; 12: 417–423. [PubMed: 8951678]
21. Yang L, Di G, Qi X, et al. Substance P promotes diabetic corneal epithelial wound healing through molecular mechanisms mediated via the neurokinin-1 receptor. Diabetes. 2014; 63:4262–4274. [PubMed: 25008176]
22. Murphy CJ, Marfurt CF, McDermott A, et al. Spontaneous chronic corneal epithelial defects in dogs: clinical features, innervation and effect of topical SP with or without IGF-1. Investigative Ophthalmology & Visual Science 2001; 42: 2252–2261. [PubMed: 11527938]
23. Kovocs I, Ludany A, Koszegi T, et al. Substance P release from sensory nerve endings influences tear secretion and goblet cell function in the rat. Neuropeptides. 2005; 39:395–402. [PubMed: 15992924]
24. Sabatino F, Di Zazzo A, De Simone L, et al. The intriguing role of neuropeptides at the ocular surface. The Ocular Surface 2017; 15: 2–14. [PubMed: 27840126]
25. Cortina MS, He J, Na L et al. Recovery of corneal sensitivity, CGRP positive nerves and increased wound healing are induced by PEDF plus DHA after experimental surgery. Archives of Ophthalmology 2012; 130 (1): 76–83. [PubMed: 21911652]
26. Marfurt CF, Murphy CJ, Florczak JL. Morphology and neurochemistry of canine corneal innervation. Investigative Ophthalmology & Visual Science 2001; 42: 2242–2251. [PubMed: 11527937]
27. Jones MA, Marfurt CF. Peptidergic innervation of the rat cornea. Experimental Eye Research 1998; 66: 421–435. [PubMed: 9593636]
28. Moller K, Zhang YZ, Håkanson R, et al. Pituitary adenylate cyclase activating peptide in a sensory neuropeptide: immunocytochemical and immunoreactive evidence. Neuroscience 1993; 57:725–732. [PubMed: 7508577]
29. Ehinger B Connections between adrenergic nerves and other tissue components in the eye. Acta Physiologica Scandinavica 1966; 67: 57–64. [PubMed: 5963303]

30. Uusitalo H, Lehtosalo J, Laakso J, et al. Immunocytchemical and biochemical evidence for 5-hydroxytryptamine containing nerves in the anterior part of the eye. Experimental Eye Research 1982; 35: 671–675. [PubMed: 6759146]

31. Osborne NN. The occurrence of serotonergic nerves in the bovine cornea. Neuroscience Letter 1983; 35:15–18.

32. Stiles J Ocular manifestations of feline viral diseases. The Veterinary Journal 2014; 201:166–173. [PubMed: 24461645]

33. Hamrah P, Cruzat A, Dastjerdi MH, et al. Corneal sensation and subbasal nerve alterations in patients with herpes simplex keratitis: an in vivo confocal microscopy study. Ophthalmology 2010; 117:1930–1936. [PubMed: 20810171]

34. Chucair-Elliott AJ, Zheng M, Carr DJ. Degeneration and regeneration of corneal nerves in response to HSV-1 infection. Investigative Ophthalmology & Visual Science 2015; 56:1097–1107. [PubMed: 25587055]

35. Cortina MS, He J, Na L, et al. Neuroprotectin D1 synthesis and corneal nerve regeneration after experimental surgery and treatment with PEDF plus DHA. Investigative Ophthalmology & Visual Science 2010; 51: 804–810. [PubMed: 19797230]

36. He J, Thang LP, Kakazu A, et al. Recovery of corneal sensitivity and increase in nerve density and wound healing in diabetic mice after PEDF plus DHA treatment. Diabetes 2017; 66: 2511–2520. [PubMed: 28592408]

37. He J, Neumann D, Kakazu A, et al. PEDF plus DHA modulate inflammation and stimulate nerve regeneration after HSV-1 infection. Experimental Eye Research 2017; 161: 153–162. [PubMed: 28642110]

38. Pham TL, He J, Kakazu AH, et al. Defining a mechanistic link between pigment epithelium-derived factor, docosahexaenoic acid, and corneal nerve regeneration. The Journal of Biological Chemistry 2017; 292: 18486–18499. [PubMed: 28972155]

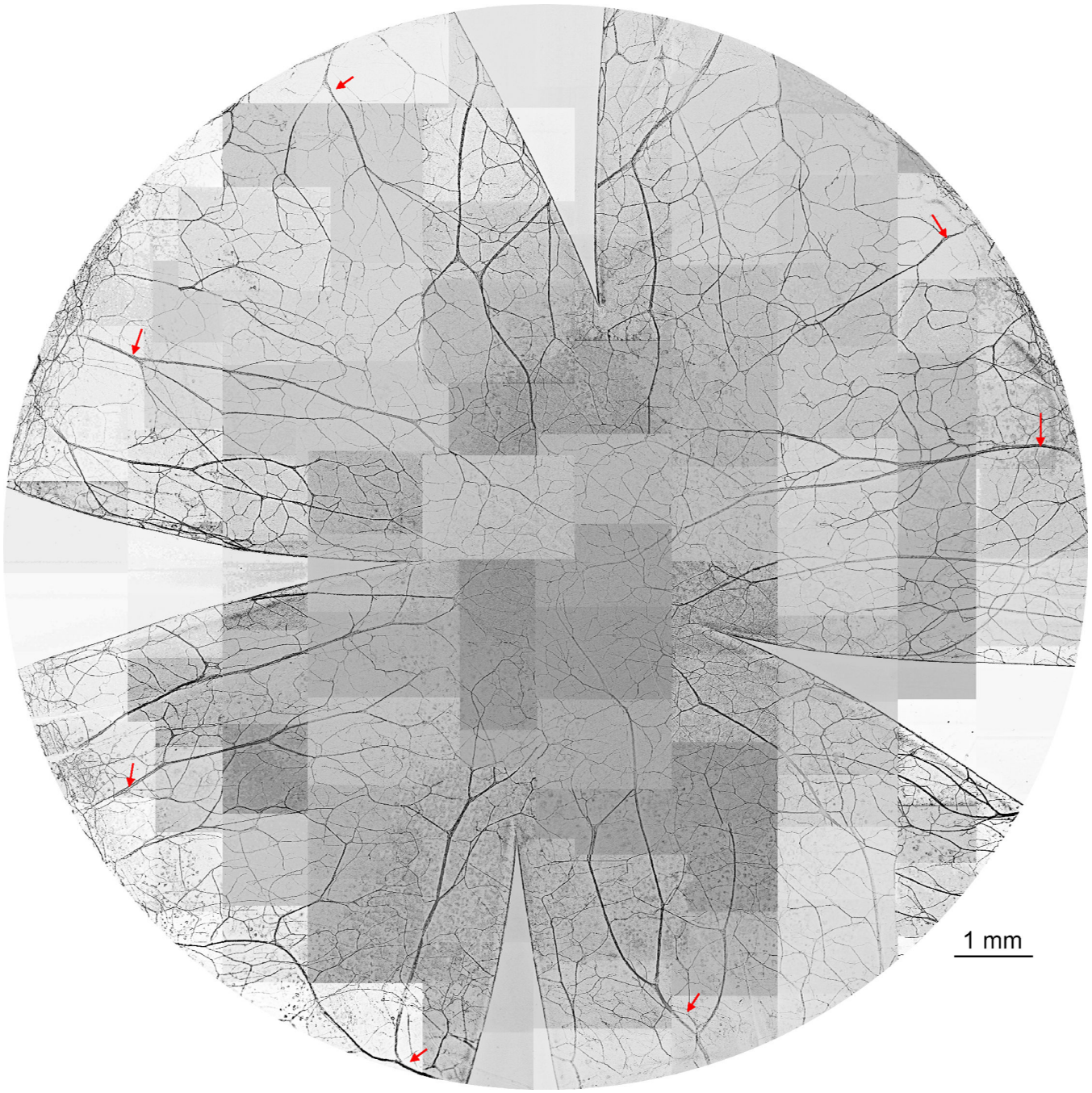

Figure 1.

Representative image of cat whole-mount corneal stromal nerves. The stromal nerves enter the cornea around the limbus as thick trunks and divide into many branches. These branches go toward the center and connect with each other to constitute the stromal nerve network. The entire cornea was labeled with PGP9.5, whole mount images were acquired using a fluorescent microscope with a 5x objective lens and images inverted to the white background. The picture was reconstructed from more than 100 images. The arrows indicate the main trunks of stromal nerves close to the limbus.

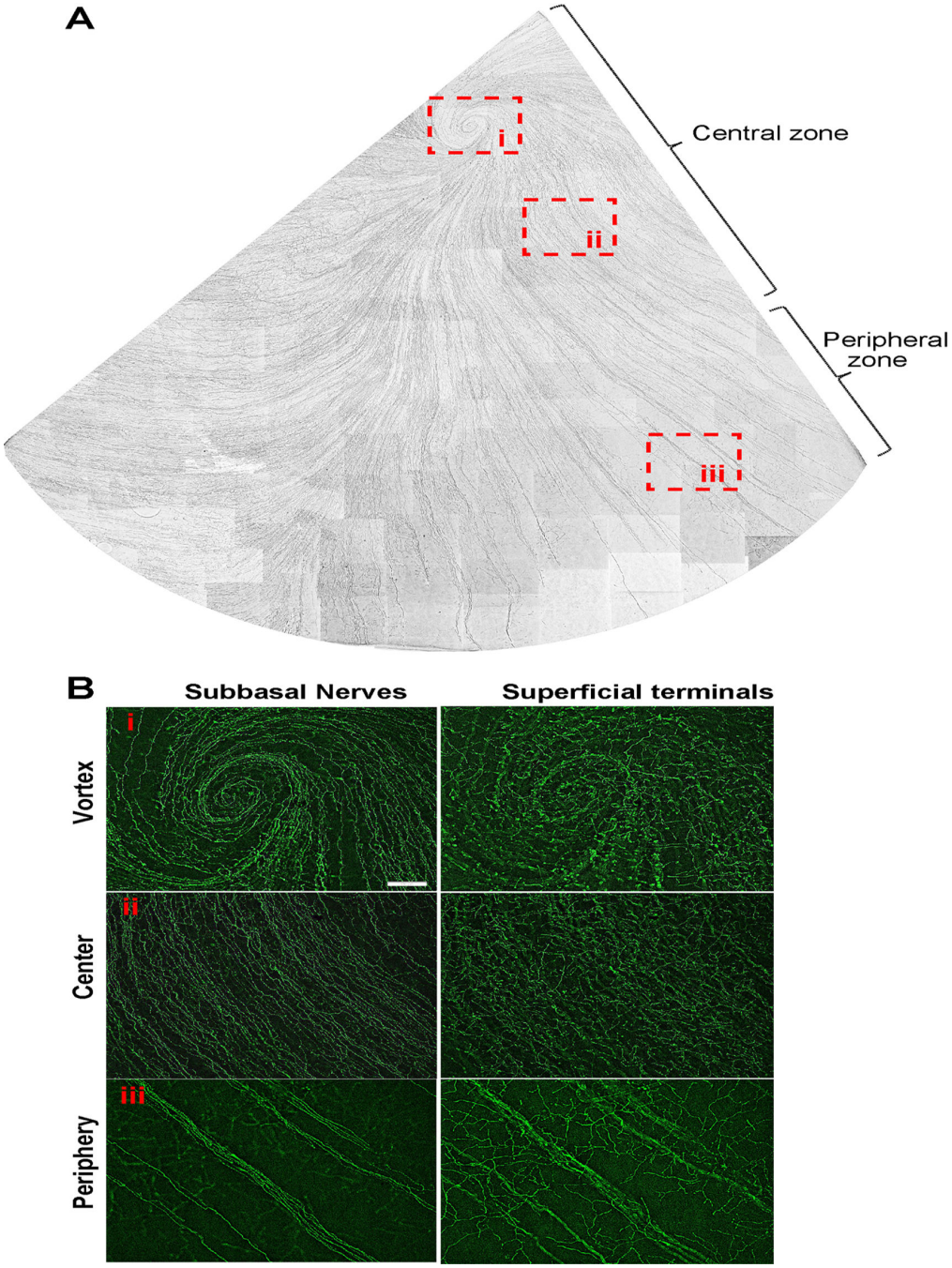

Figure 2.

Whole-mount view of epithelial nerves from a quarter of cat cornea. Images were acquired in time-lapse mode with a 10x objective lens. A) Subbasal nerves; B) Highlighted images as framed in A) show the detailed structures of subbasal nerves and terminals at the vortex (i), center (ii), and periphery zones (iii) of cat cornea.

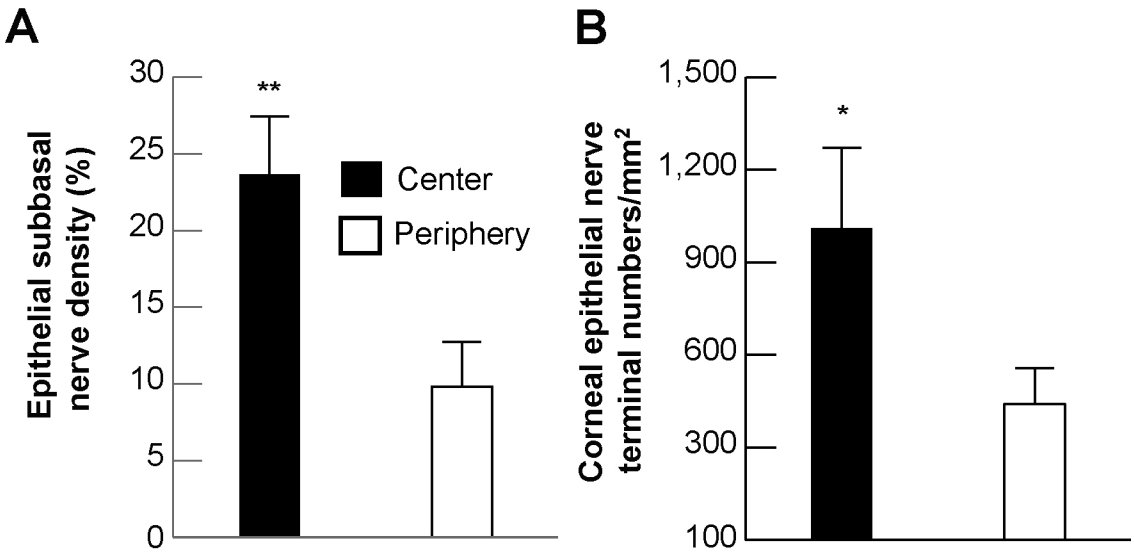

Figure 3.

Subbasal nerve density and number of nerve terminals in the center and periphery. A) Subbasal nerve density was calculated as percentage of total area in each image. Sixteen images from each zone of four corneas were used. B) The terminal numbers in each image (16 images/zone) were directly counted. Each image took up an area of 0.59 mm^2, and the terminal numbers per mm^2 were calculated. Data were expressed as average ± SD. Significant differences *$p<0.005$ and **$p<0.001$ between center and periphery zones.

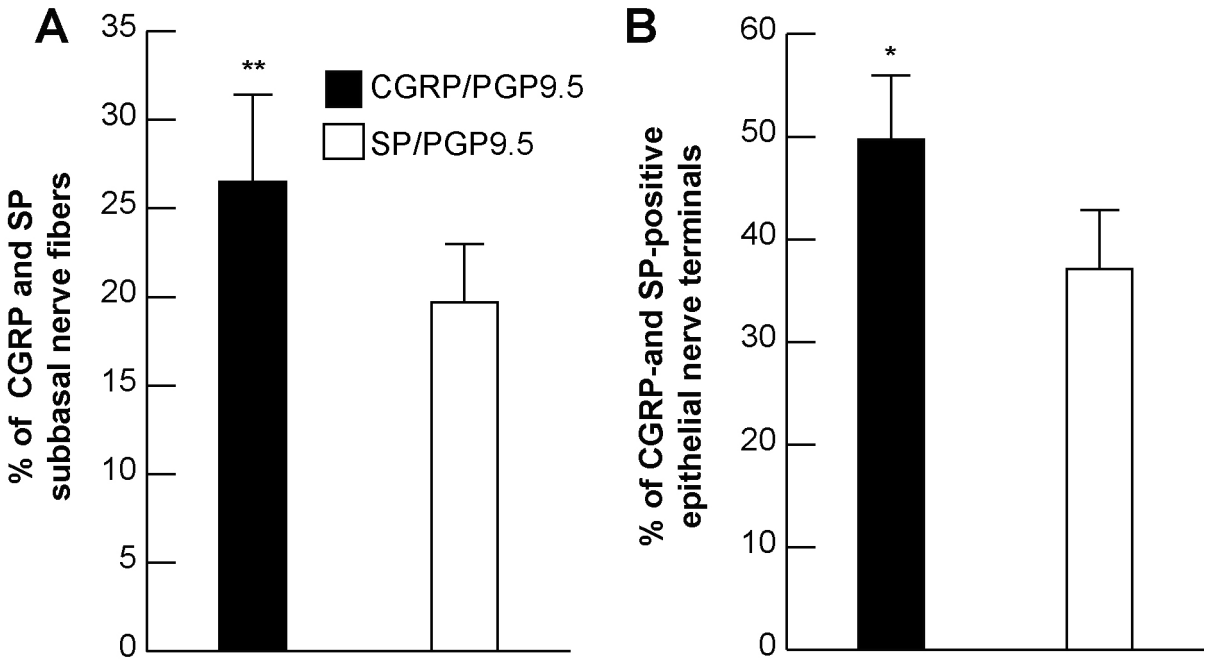

Figure 4.

The relative content of sensory neuropeptides in cat corneal epithelium. Percentage calculated as ratios of CGRP- and SP-positive subbasal epithelial nerves A) and nerve terminals B) versus total nerve area (PGP9.5-positive nerves) in each image. A total of 16 images for each neuropeptide and the same number of images for PGP9.5 were recorded from 4 corneas. Data expressed as average ± SD. *p<0.005, **P<0.001.

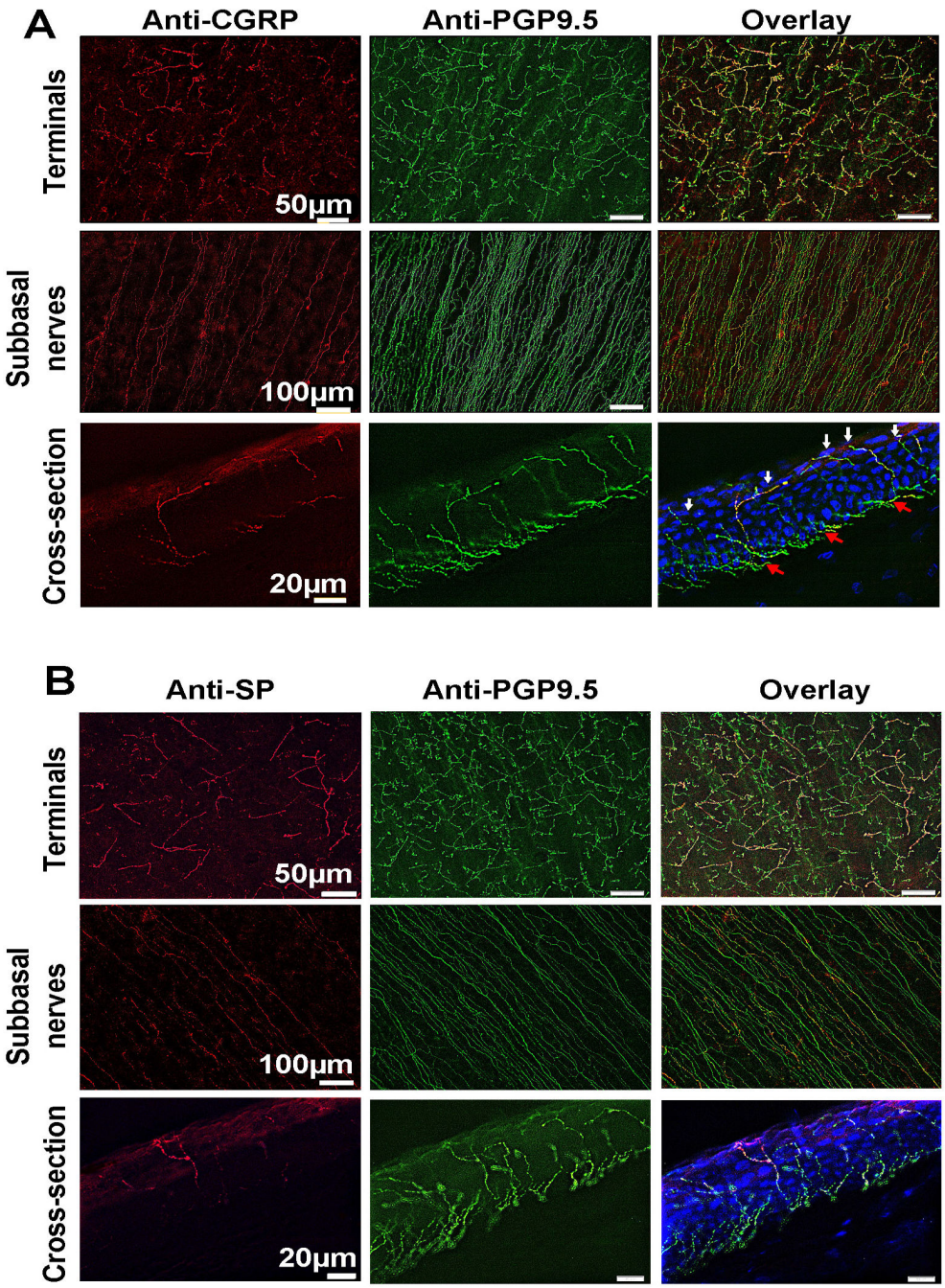

Figure 5.

Representative whole-mount and cross-section images in A) and B) show the expression of CGRP- and SP-positive nerves in the central subbasal bundles and terminals. In the cross-sections, DAPI (blue) was used to counterstain cell nuclei; red arrows show the subbasal nerves; white arrows indicate the terminals.